# Experimental observation of Rainbow Trapping of water waves

Aidan Archer[1], Hugh Wolgamot[1,†], Jana Orszaghova[1],
Luke G. Bennetts[2], Malte A. Peter[3], Richard V. Craster[4]

[1]The University of Western Australia, WA 6009, Australia, [†]hugh.wolgamot@uwa.edu.au
[2]School of Mathematical Sciences, University of Adelaide, SA 5005, Australia
[3]Institute of Mathematics, University of Augsburg, 86135 Augsburg, Germany
[4]Department of Mathematics, Imperial College London, London SW7 2AZ, UK

## Introduction

At the workshop in Guidel-Plages in 2018, Peter et al. (2018) demonstrated rainbow trapping of water waves in arrays of bottom-mounted cylinders, using linear potential flow theory. The array arrangements were finite chirped arrays, with lattice spacing increasing in the direction of the incident wave. The incident wave in such arrays is amplified when it reaches a region inside the grating where its effective group velocity vanishes and the incident energy therefore accumulates. Different frequencies are amplified in different parts of the array, leading to the phenomenon being referred to as rainbow trapping in the wider literature, e.g. in acoustics. This idea could be used to increase the efficiency of wave energy converters in the ocean, perhaps for arrangements of chirped resonators like those discussed in Bennetts et al. (2018). This represents a departure from the study of regular arrays, which have been extensively studied in the literature.

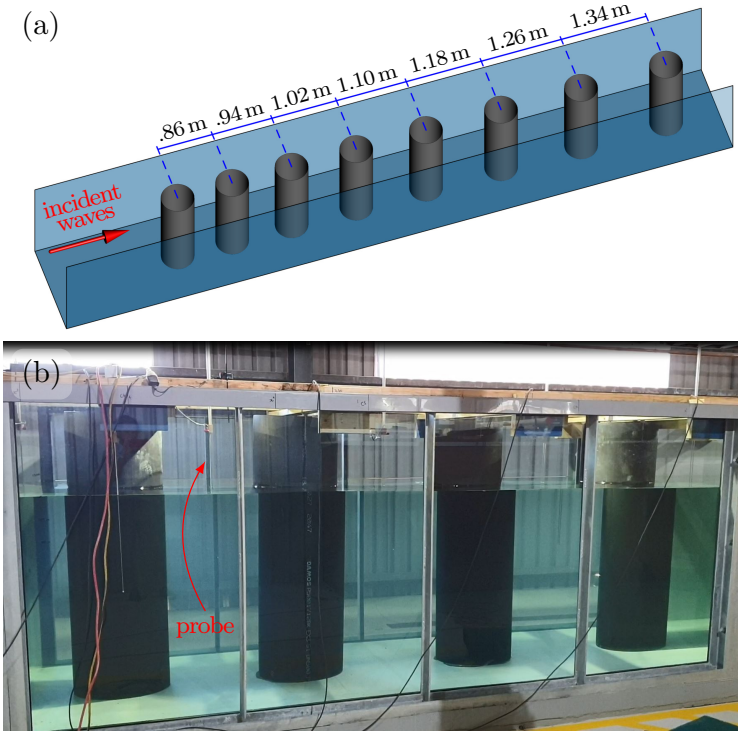


Figure 1: (a) Wave flume experimental set-up, involving a chirped array of eight identical cylinders, with spacing increasing in the incident wave direction. (b) Side-view photo showing cylinders 3–6, including probes in cylinder gaps.

Here we present experimental tests of a chirped array of 8 bottom-mounted circular cylinders placed along the centreline of a wave flume at UWA (Fig. 1). The cylinders are of 0.5 m diameter, the flume width is 1.49 m, the water depth 1.1 m and the chirp changes the centre-to-centre spacing from 0.86 m (first gap) to 1.34 m (final gap) – see Fig. 1. Surface elevations are measured at the centre of each gap in the array (except the last), and at a point halfway between the first cylinder and the the bottom-hinged wavemaker approximately 22 m away. Waves which pass through the array are absorbed by a porous planar beach (of slope 1:10) at the far end of the flume.

## Theoretical context

As in Peter et al. (2018) we produce band diagrams from periodic arrays, here setting the lateral ($y$) spacing equal to the distance between the flume walls. Fig. 2(a) shows the band diagram when the periodicity in the $x$-direction is set by the third gap in the array. Four band gaps (defining frequency ranges where waves cannot propagate) are identifiable, we focus on the second. Fig. 2(b) is a representation of how this band gap changes along the finite chirped array tested.

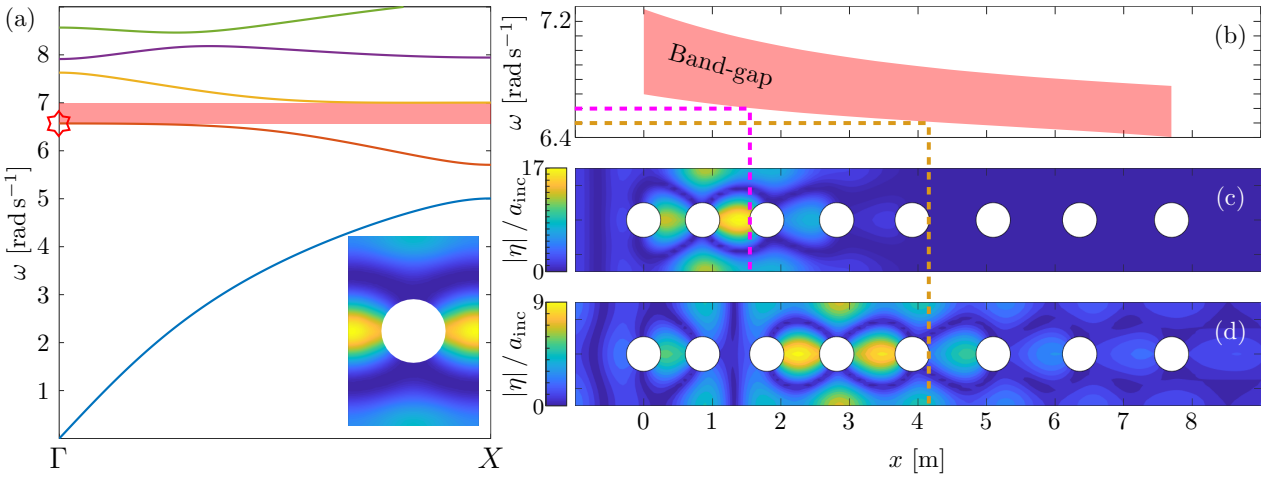


Figure 2: (a) Band diagram of symmetric modes for infinite array, using third cylinder gap for $x$-periodicity, where the abscissa covers wavenumber space for normal incidence in the first irreducible Brillouin zone and red shading indicates second band-gap. Inset shows eigenmode on second band at $\Gamma$, as indicated by red star. (b) Red shading shows evolution of the second band-gap as cylinder gaps increase along the array, where spacing is interpolated between gap mid-points and extrapolated at ends. (c,d) Model predictions of free surface elevation modulus, $|\eta|$, normalised by the incident amplitude, $a_{\mathrm{inc}}$, for regular incident waves with angular frequency (c) $\omega = 6.60\,\mathrm{rad\,s^{-1}}$ and (d) $\omega = 6.50\,\mathrm{rad\,s^{-1}}$. Dashed curves connecting (b) with (c,d) indicate theoretical predictions of zero group velocity, where $\omega = 6.60\,\mathrm{rad\,s^{-1}}$ (- -) and $\omega = 6.50\,\mathrm{rad\,s^{-1}}$ (- -) enter the band-gap.

For the finite array we use Hydrostar, with the tank walls accounted for (Chen, 1994), to produce the plots in Fig. 2(c) and (d), where it is shown that for different incident frequencies the maximum amplification in the array occurs slightly upwave of the edge of the band gap. These results demonstrate the power of the band gap predictions (based on local periodicity) to explain and interpret the phenomena occurring in chirped arrays.

## Experimental Rainbow Trapping

We seek to demonstrate rainbow trapping by observing different frequencies being amplified in different sections of the array. To do this we excite the array with wave groups spanning the frequency range of interest, which are of the form

$$\eta_{\mathrm{inc}}(\tau) = \frac{a_{\mathrm{inc}} \sum_n \{S(\omega_n)\, \cos(k_n\, x_0 - \omega_n\, \tau)\}}{\sum_n S(\omega_n)}, \tag{1}$$

where $a_{\mathrm{inc}} = 0.045\,\mathrm{m}$ is the nominal amplitude, $x_0 = -24\,\mathrm{m}$ is the mean wavemaker position relative to the linear focal point, $\tau$ is time relative to linear focus time, $k_n$ is the wavenumber, and $S$ is a Gaussian with standard deviation $\sigma = 0.15\,\mathrm{rad\,s^{-1}}$ and mean $\omega_{\mathrm{p}} = 6.03\,\mathrm{rad\,s^{-1}}$, i.e. a frequency just below the second band gap. The linear focus position is 2 m into the array and the sum is over $2^{10}$ equally spaced components.

Fig. 3 displays the linear transfer function from incident to scattered wave at the centre of each cylinder gap (excluding the last). The left plot (panel a) is determined numerically, while the right

plot (panel b) is experimentally derived. The incident waves are also run without the cylinders in the tank and the linearisation is accomplished using the phase combination method – see, e.g. Fitzgerald et al. (2014).

It is apparent that the broad 'rainbow trapping' amplification structure associated with the first two band gaps (starting at around 5 and 6.75 rad s$^{-1}$, respectively, in the first cylinder gap) seen in the numerics is reproduced in the experiments. Also seen (less clearly) is the very low transmission associated with the band gaps themselves.

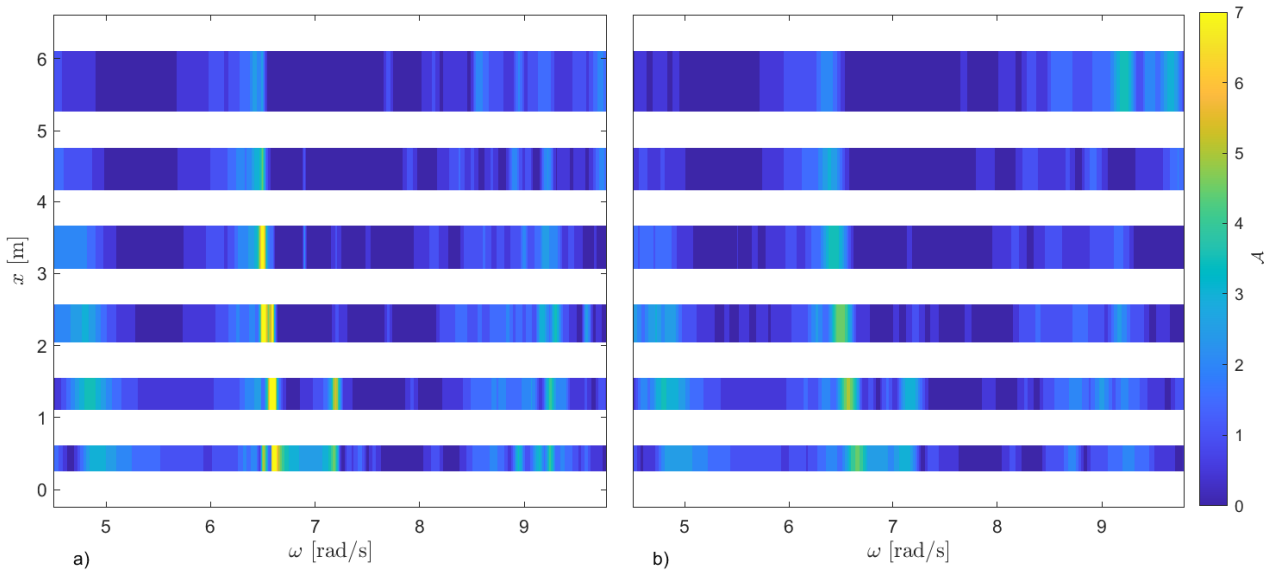


Figure 3: (a) Numerical and (b) experimental amplitude transfer functions, at wave probe locations along the array (shown as constant in each cylinder gap). White areas represent spatial locations of cylinders 1–7.

## Resonant behaviour

In Fig. 3 the colour axis is truncated to ensure that the broad-scale structure can be seen. However, as Fig. 2 shows, the peaks in the response within the array are highly resonant. This presents challenges for the experimental testing. The timescales of these highly resonant modes are much longer than the timescale for reflections to occur from the wave paddle in the flume (active absorption cannot be used because the paddle is a single element and the reflected field is non-planar).

Hence, decay of the response to a focussed wave group, or the build-up in the response to an incident regular wave (aligned with one of the band gaps) is corrupted by reflected signals after a relatively short time. This makes it challenging to assess the magnitude of the resonant responses that would be achieved in an 'uncontaminated' experiment in the absence of reflections (but with viscous damping, nonlinearity, etc). The slow decay of the resonant motions is also challenging because, without active absorption enabled in the flume, the major source of dissipation is viscous damping on the walls (the beach being exposed to relatively little energy at the resonant frequencies due to the band gap preventing transmission). This entails long wait times between experiments, even when additional porous dampers are lowered into the flume to assist.

Using the recorded paddle motion (with a linear ramp over 11 periods) and the method presented in Eatock Taylor (2007) incident regular wave transients observed in the flume can be recreated and the numerical transfer functions used to produce synthetic time series of the build-up in response to the regular wave forcing. A comparison between the numerical and experimental responses in the second cylinder gap, when driven by a wave of frequency 6.60 rad s$^{-1}$ (i.e. corresponding to Fig. 2c) is given in Fig. 4. Here, the experimental responses are linearised by band-pass filtering; this is necessary as considerable higher harmonics, including a mean offset of the free surface, build up as the response amplitude increases. The window shown in Fig. 4 is truncated just before the arrival of reflections,

but it is apparent that neither the experimental nor numerical curves are approaching steady state. Some additional damping is apparent in the experimental data, as expected. What is not easily seen is the slow modulation of the build-up envelope due to the resonant peaks in adjacent cylinder gaps – this makes extrapolation to steady state on the basis of a limited record more difficult.

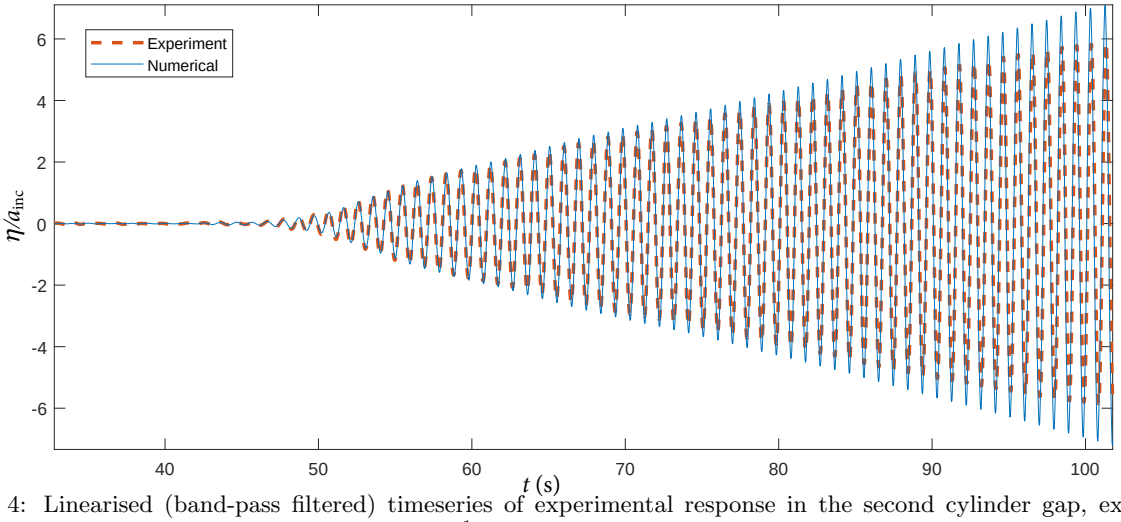


Figure 4: Linearised (band-pass filtered) timeseries of experimental response in the second cylinder gap, excited by an incident regular wave of frequency 6.60 rad s$^{-1}$ and amplitude $a_{\mathrm{inc}} = 0.01$ m, with corresponding linear numerical prediction of the same response.

## Discussion

In this paper we have presented experimental observations of rainbow trapping in water waves. The chirped array tested was not optimised in any meaningful sense, and there is much work to do to explore such optimisation.

At the workshop further results associated with the first band gap, additional amplitude and frequency experiments and more extensive conclusions will be presented.

## Acknowledgements

AJA was supported by the Wave Energy Research Centre, jointly funded by The University of Western Australia and the Western Australian Government, via the Department of Primary Industries and Regional Development (DPIRD). HAW acknowledges financial support from Shell Australia. LGB is supported by an Australian Research Council mid-career fellowship (FT190100404). RVC thanks the UK EPSRC for their support through Programme Grant EP/L024926/1 and also acknowledges the support of the Leverhulme Trust.

## References

L. G. Bennetts, M. A. Peter, and R. V. Craster. Graded resonator arrays for spatial frequency separation and amplification of water waves. *J. Fluid Mech.*, 854:R4, 2018.

X. Chen. On the side wall effects upon bodies of arbitrary geometry in wave tanks. *Appl. Ocean Res.*, 16(6):337–345, 1994.

R. Eatock Taylor. On modelling the diffraction of water waves. *Ship Technol. Res.*, 54(2):54–80, 2007.

C. J. Fitzgerald, P. H. Taylor, R. Eatock Taylor, J. Grice, and J. Zang. Phase manipulation and the harmonic components of ringing forces on a surface-piercing column. *Proc. Roy. Soc. Lond. A*, 470(2168):20130847, 2014.

M. A. Peter, L. G. Bennetts, and R. V. Craster. Rainbow trapping of water waves. In *Proc. 33rd Int. Workshop on Water Waves and Floating Bodies, Guidel-Plages, France (ed. Y.-M. Scolan)*, pages 157–160, 2018.